

# AFM Studies of Molecular Packing in Fatty Acid Langmuir-Blodgett Films

Daniel K. Schwartz  
Department of Chemistry, Tulane University  
New Orleans, LA 70118

Ravi Viswanathan and Joseph A. Zasadzinski  
Department of Chemical and Nuclear Engineering  
University of California  
Santa Barbara, CA 93106

**Abstract.** By careful calibration and by minimizing piezoelectric scanner drift and nonlinearity we have achieved sufficient precision to study surface crystallographic structures of Langmuir-Blodgett (LB) films using the atomic force microscope. In studying the molecular packing of LB films made from divalent salts of the n-alkanoic acids we have discovered a general correlation between packing density and the electronegativity of the cation. In addition, we have observed two distinct types of spatially modulated structures (on nanometer length scales) on the surface of these films. Both involve periodic height modulation of the crystalline molecular lattice. The first type, seen in films containing  $\text{Ba}^{++}$ ,  $\text{Ca}^{++}$ , and  $\text{Mg}^{++}$ , is commensurate with the molecular lattice and can be described as a regular series of packing defects that are consistent with the close-packing requirements of the alkyl tail groups. The other type, seen in films containing  $\text{Cd}^{++}$  and  $\text{Mn}^{++}$ , is not always commensurate and is less perfectly correlated than the first type. We suggest a correspondence between these two types of modulations and the two predicted by a new theoretical model which incorporates the competition between the in-plane density preferred by the headgroups in conjunction with the cation and the close-packing requirements of all- *trans* crystalline alkyl chains.

## 1. Introduction

Much of the behavior associated with amphiphilic molecules can be traced to the inherent competition between the hydrophilic headgroups and hydrophobic tailgroups of these molecules. For example, the tendency to form micellar versus lamellar structures in solution can be related to the relative cross-sectional areas of head versus tail [1]. When surfactant molecules are constrained to lie in a plane, the nature of the competition between heads and tails becomes particularly clear. For example, if the heads have a larger cross section than the tails, the molecules will tilt away from the substrate normal to simultaneously satisfy both. Figure 1 shows that a simplified surfactant molecule (with a cylindrical tail) whose heads prefer a separation  $b$  and whose tails prefer a separation  $a$  (with  $a < b$ ) will tilt at an angle of  $\theta$  such that  $\cos\theta = a/b$ . However, real tails such as the alkyl chains often used, are not well-described by cylinders and hence will not willingly pack at an arbitrary angle defined by this relation. In fact, as demonstrated in Figure 2, there are only certain discrete angles at which (all *trans*) alkyl chains will comfortably pack. In two dimensions the picture is more complicated since several close-packing structures of alkanes are known [2]. However, even considering the various discrete tilt angles allowed for all of the classes of packing, the fact remains that not every headgroup can be easily accommodated by a uniform crystalline alkane structure. The question we explore in this report is: what structure will result when the headgroup prefers a packing density which is not consistent with uniform alkane close-packing ?

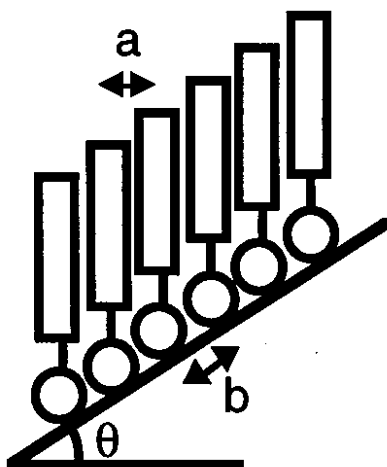


**Figure 1.** Uniformly tilted film of surfactant molecule with featureless tails. The tails are assumed to prefer to pack with a spacing  $a$  and the heads with a spacing  $b$ . Both are satisfied by tilting by an angle  $\theta$  such that  $\cos\theta = a/b$ . The straight line represents the substrate plane. It is drawn tilted for simplicity.

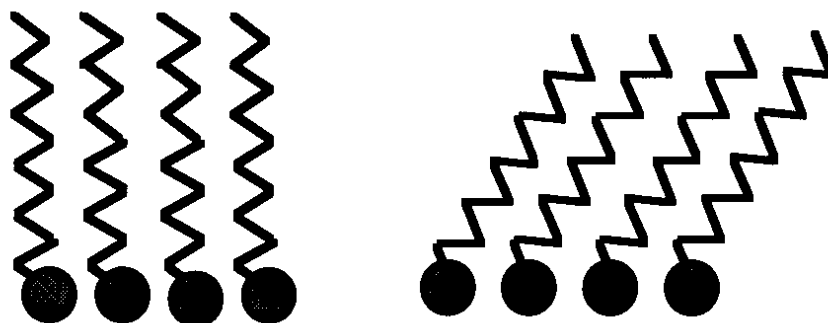


**Figure 2.** Crystalline alkanes have several distinct forms of close-packing. The chains may point in the direction of the layer normal or they may tilt away from the normal in a lattice symmetry direction. The tilt must be by certain discrete angles that preserve the nesting of the chains.

## 2. Experimental

A straight chain fatty acid  $\text{CH}_3(\text{CH}_2)_n\text{COOH}$  ( $n=16,18,20,22$ , Aldrich, 99%) was spread from chloroform solution (Fisher spectranalyzed) onto a 0.5 mM solution (water from a Millipore Milli-Q UV+ system) of the chloride salt of a particular cation ( $\text{Ba}^{++}$ ,  $\text{Ca}^{++}$ ,  $\text{Mg}^{++}$ ,  $\text{Cd}^{++}$  or  $\text{Mn}^{++}$ , from Aldrich 99%). The pH was adjusted using  $\text{NaHCO}_3$  or  $\text{NaOH}$  (Aldrich 99%) in order to have the acid completely dissociated. The films were transferred to solid substrates by successive vertical dipping (a NIMA trough was used) at 1.6 mm/min at  $T=22.0\pm 0.5$  °C and  $\pi=30.0 \pm 0.1$  mN/m. Substrates were polished silicon oxide, crystalline silicon (100), or mica. The details of film deposition have been previously reported [3]. Imaging was performed using a Nanoscope II or III (from Digital Instruments) in "force mode" in ambient conditions using a  $1\mu\text{m} \times 1\mu\text{m}$  scan head and a silicon nitride tip on an integral cantilever with spring constant 0.12 N/m. By careful calibration, eliminating drift, and statistical analysis procedures, we were able to quantitatively determine the two-dimensional crystal structure of the surface molecules with a precision of about  $\pm 1\%$ . Further details of imaging and analysis have been previously reported [4].

### 3. Results

As Figure 3 demonstrates, the counterion plays the dominant role in determining the overall packing density of the film. We previously concluded that counterions that bind more or less covalently with the acid (like  $\text{Cd}^{++}$ ) induce the headgroups to pack tightly together [3, 5]. In fact, the molecular area of  $18\text{\AA}^2$  for Cd-containing films is the limiting cross-sectional area of an alkane chain. Films with counterions that interact electrostatically with the acid, such as  $\text{Ba}^{++}$  or  $\text{Ca}^{++}$  have correspondingly expanded lattices. We can presume, in these cases, that the headgroups retain some repulsive interaction not completely screened by the cation. The Pauling electronegativity is a rough guide to the degree of covalent versus ionic bonding in this case and Figure 3 shows that there is a good correlation between electronegativity and two-dimensional density. Therefore, by simply changing the cation in the subphase we can explore the response of the alkyl tails to a changing density constraint imposed by the headgroup.

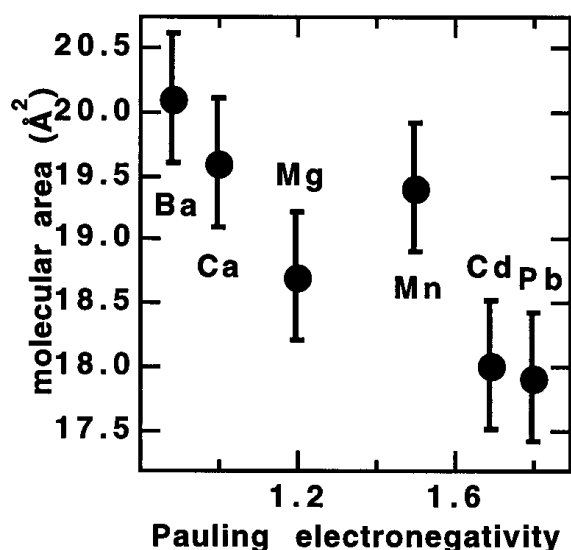


**Figure 3.** Two-dimensional density of LB films containing different counterions. The cations that bind more covalently like  $\text{Cd}^{++}$  and  $\text{Pb}^{++}$  induce the surfactant molecules to pack densely. Cations like  $\text{Ba}^{++}$  and  $\text{Ca}^{++}$  that interact electrostatically produce less densely packed films. The density of the film can, therefore, be tailored over the region  $18\text{-}20\text{ \AA}^2/\text{molecule}$ .

Figures 4a,c,e show molecular resolution images of the dominant structures found on films of  $\text{Ba}^{++}$  [6-8],  $\text{Ca}^{++}$  [9] and  $\text{Mg}^{++}$  [5] fatty acid salts respectively. In all three cases, there is a superstructure that results in the unit cell being larger than one molecule in at least one dimension. The Fourier transforms (FT), in figures 4b,d,f respectively, clearly show that the bright spots corresponding to the distance between molecular rows is exactly the third, fourth, or second harmonic respectively of the FT spot corresponding to the superstructure periodicity (marked by arrows). Furthermore, the molecular packing in all three cases is consistent with models based on the well-known "ideal" packing [2] of alkane chains shown in Figures 5a-c [6, 7, 9, 10]. In each case, the unit cell is constructed by inserting a regular series of packing defects into some form of the "ideal triclinic" alkane packing. The defects are also consistent with alkane close-packing. In fact the packing in the defects themselves are related to the packing in the uniform regions between defects by mirror symmetry (the triclinic is a chiral packing). The defects also contain a component along the chain direction and hence serve to alter the overall density and tilt angle from those of the uniform triclinic structure. Figure 6 shows a simplified one-dimensional cartoon that clarifies this point. For example, if

the film containing Ba had no defects, the molecular area would be  $21.1 \text{ \AA}^2$  (Kitaigorodskii's [4] T[1/2 1]); the defects reduce it to  $20.4 \text{ \AA}^2$ . Similarly, the defects in the film with Ca increase the molecular area from  $18.9 \text{ \AA}^2$  (T[1/2 0]) to  $19.7 \text{ \AA}^2$  and in the Mg-containing films the area is decreased from  $18.9 \text{ \AA}^2$  (T[1/2 0]) to  $18.2 \text{ \AA}^2$  by the defects. The key point is that none of the favorable van der Waals interaction between alkyl chains is sacrificed by having these defects because they simply represent the mirror image of the packing. We, therefore, label these modulations "locked modulations" because the defects are locked into the molecular corrugations of the tails.

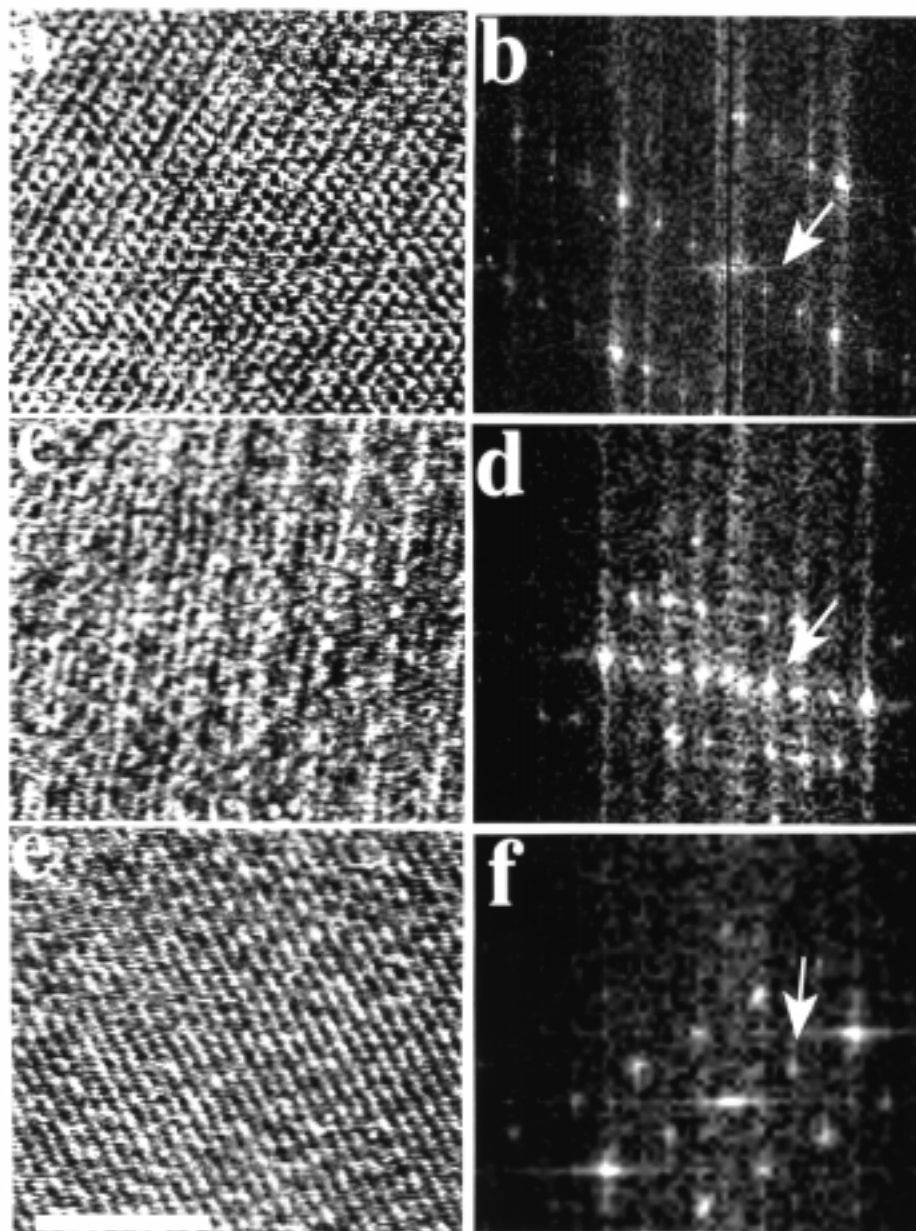


**Figure 4.** Un-enhanced molecular resolution images of 3 layer thick (a) barium arachidate, (c) calcium arachidate and (e) magnesium stearate LB films along with their Fourier transforms, (b), (d), and (f) respectively. The arrows refer to the Fourier spot that represents the modulation wavelength. The bright spots that represent the approximate inter-molecular spacings are the third, fourth, and second harmonics respectively. The bar represents 5 nm.

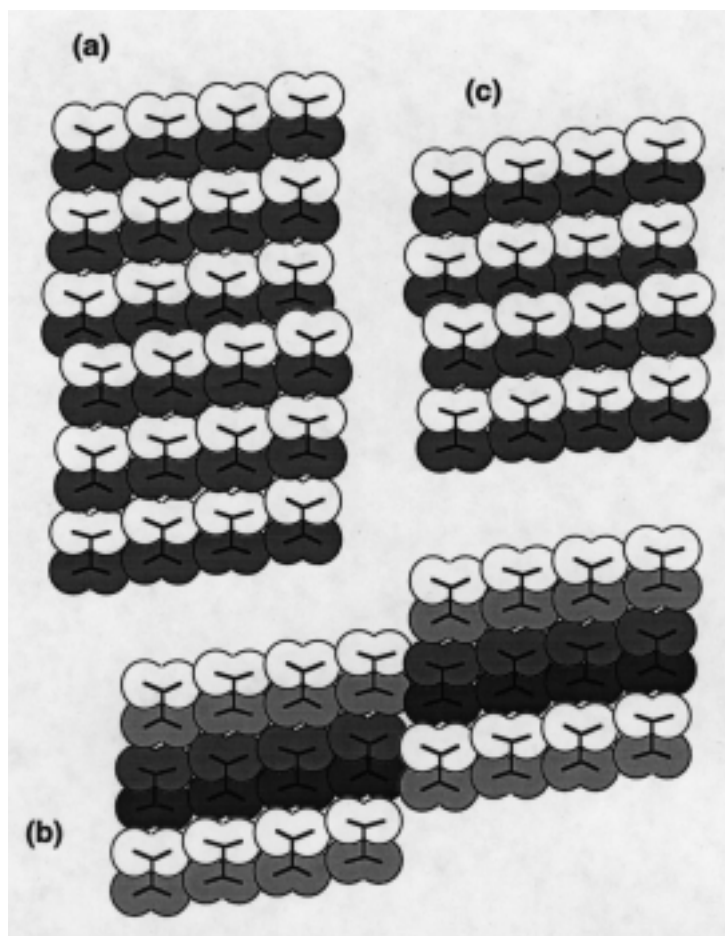


**Figure 5.** (a-c) Molecular models showing how periodic packing defects account for the modulations shown in figures 4a, 4c, and 4e respectively. All three structures are locally based on the triclinic form of close-packing. However, periodic defects which reverse the local packing chirality serve to adjust the tilt (and therefore in-plane density) to that preferred by the particular cation.

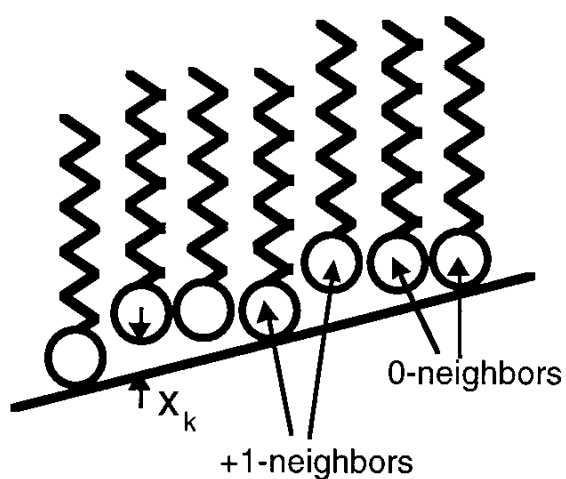


**Figure 6.** The periodic inclusion of packing defects can change the average tilt angle and, therefore, the in-plane density of a film. The regions of untilted phase (0-neighbor) are interrupted by defects (+1-neighbors) resulting in a less dense tilted film. The molecules must translate along their length to achieve the preferred packing, this translation is labeled by the variable  $x_k$ .

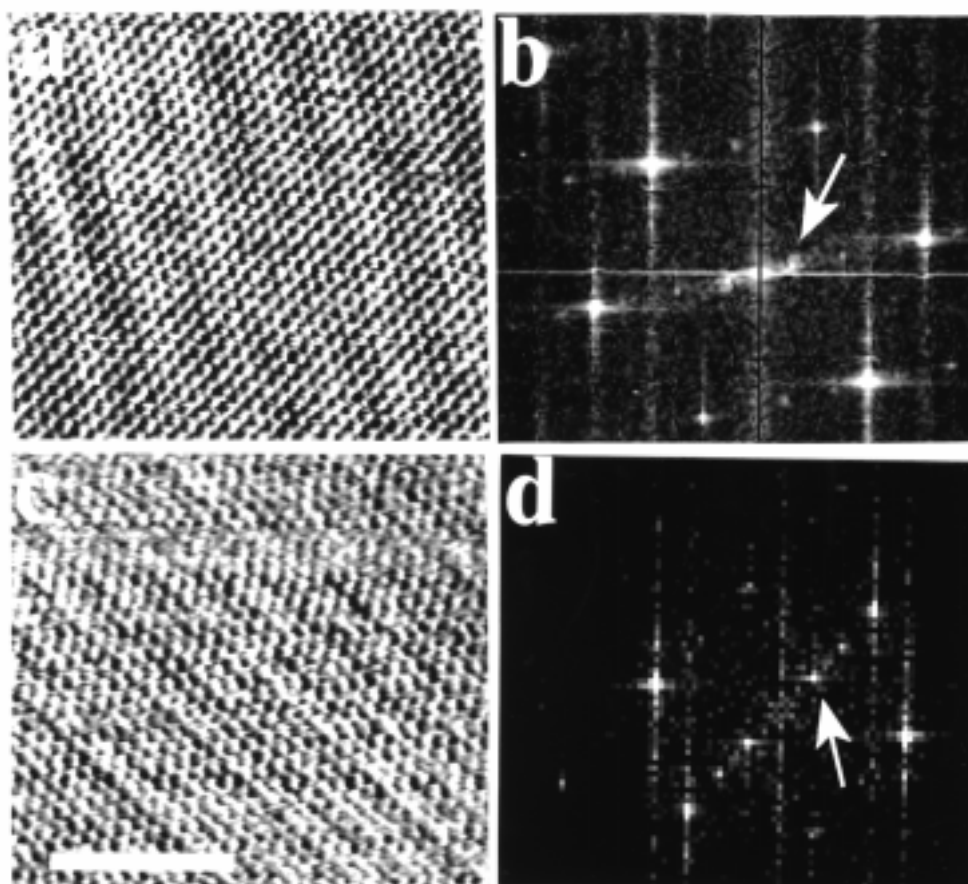


**Figure 7.** Molecular resolution images of 3 layer (a) cadmium arachidate (CdA) and (c) manganese arachidate (MnA) LB films along with their Fourier transforms, (b) and (d) respectively. The arrows refer to the Fourier spot that represents the modulation wavelength. The bright spots that represent the molecular spacing are not exact multiples of the modulation period. The bar represents 5 nm.

The periodic height modulations observed in films containing  $\text{Cd}^{++}$  [11, 12] and  $\text{Mn}^{++}$  [3, 5] however, differ in several ways from these locked modulations (see Figure 7). In both cases, the molecular area and packing is consistent with one or another "ideal" uniform packing of alkane chains. In the case of  $\text{Cd}^{++}$  the chains are in the untilted rectangular "herringbone" arrangement (Kitaigorodskii's  $R[0\ 0]$ ) and in the case of  $\text{Mn}^{++}$  the chains are in a uniformly tilted rectangular packing ( $R[0\ 1]$ ). Therefore, the modulation doesn't result in a measurable change in density from an ideal alkane packing. Also, the wavelength of the modulation is not always an exact multiple of the molecular periodicity. In fact, there are significant variations in the modulation period from region to region in a film [10]. There is a subtle increase in modulation wavelength with increasing chain length. However, the width of the wavelength distribution increases markedly with increasing chain length indicating increasing disorder. In fact, for cadmium behenate (C22) films the wavelength distribution is so broad that an average periodicity cannot easily be determined. The height modulation in this case is best described as "broadband" buckling along the [10] crystal direction.

#### 4. Discussion and Theory

There have been several theoretical attempts to explain modulated or "rippled" structures in surfactant and liquid crystal systems [13-16]. Some of these theories incorporate substantial alkyl chain disorder which is difficult to reconcile with the perfect two-dimensional crystallinity we observe and the fact that the particular molecular packings observed are consistent with bulk alkane crystalline packing. These theories explain certain features of the ripple phase quite well, such as the approximately proportional dependence of the modulation period on chain length. However, as we have demonstrated, the modulations we observe have a much weaker chain length dependence. We believe that the geometrical constraints of the LB films (i.e. that they are confined to a plane) play an important role in causing the modulations and that the modulations are not entropy-driven (as are the ripple phase and modulated smectic B phases) but indicative of a ground state caused by competing length scales.

Using our experimental observations as a guide we construct a one-dimensional model that incorporates the competition between head and tail packing. As in Figure 1, we assume a surfactant molecule with heads that like to pack with a characteristic separation of  $b$  and tails with a separation of  $a$  such that  $b > a$ . The overall tilt angle must be  $\theta$ , where  $\cos\theta = a/b$ . We will assume that the major perturbation from the uniformly tilted film will be molecular translation along the molecular direction and call the translation of the  $k$ th molecule  $x_k$ . This is strongly motivated by the experimental observations. Scaling the lengths such that both the repeat distance along the alkyl chain and the distance between neighboring molecules are equal to 1, we write down the following one-dimensional Hamiltonian for the system:

$$NH = \sum_{k=0}^N x_k^2 - W \sum_{k=1}^N \sum_{l=-L/2}^{L/2} \frac{L-2|l|}{L} \exp\left(\frac{-1}{2\sigma^2} (x_k - x_{k-1} + \tan\theta - l)^2\right)$$

where  $N$  is the number of molecules and  $L$  is the number of methylene groups in the alkyl chain.

The first term tries to keep the molecules in the uniformly tilted structure. Physically, it can be regarded as an energy that disfavors deviations from flatness; if the surface undulates then some molecule must be compressed or stretched. The second term is a two-body term that takes into account the nesting of neighboring alkane chains. The sum over  $l$  represents the discrete ways in which neighboring alkanes can close-pack. The  $l=0$  term represents the potential minimum where neighboring molecules are exactly side-by-side. The  $l=1$  term represents the potential minimum where a molecule is displaced by an alkane chain repeat distance relative to its neighbor; the prefactor accounts for the decrease in van der Waals interactions due to the fact that the chains are no longer completely overlapping. When neighboring molecules are displaced by exact multiples of the chain repeat distance we can label them by that multiple (see Figure 6). The parameter  $W$  represents the relative strength of the tailgroup-tailgroup interaction compared to some other interaction like the headgroup-headgroup interaction. The parameter  $\sigma$  adds some flexibility to the restriction that neighboring molecules must fit into each other exactly.

As we shall see, Monte Carlo simulations using this Hamiltonian consistently give sawtooth solutions where neighboring molecules were displaced by the distances preferred by the alkyl chains most or all of the time. Therefore, we study the following simplified Hamiltonian:

$$NH = \sum_{k=0}^N x_k^2 - W \sum_{k=1}^N [\delta_{x_k + \tan\theta, x_{k-1}} + \delta_{x_k + \tan\theta, x_{k-1} + 1}]$$

using the following sawtooth trial solution with a period of  $n$  molecules:

$$x_k = (k \bmod n - (n-1)/2) \tan\theta.$$

We have eliminated the parameter  $\sigma$  by changing the gaussians to Kronecker delta functions. Also, since we will restrict (for now) the value of  $\theta$  such that  $0 < \tan\theta \leq 1/2$ , we need only consider the first two delta functions (at  $T = 0$ ). Finally, we neglect the prefactor which is appropriate in the limit of long molecules. This simplified Hamiltonian is no longer so model dependent. It assumes only that there are two distinct types of nearest neighbor packings that are preferred. One results in a less dense structure than the headgroups prefer while the other results in a more dense structure. The trial function is such that the first  $n-1$  neighbors of each modulation are  $0$ -neighbors. In general, the  $n$ th neighbor will not have any special character. However, if  $\tan\theta = 1/n$ , the  $n$ th neighbor will be a  $+1$ -neighbor (see Figure 8).

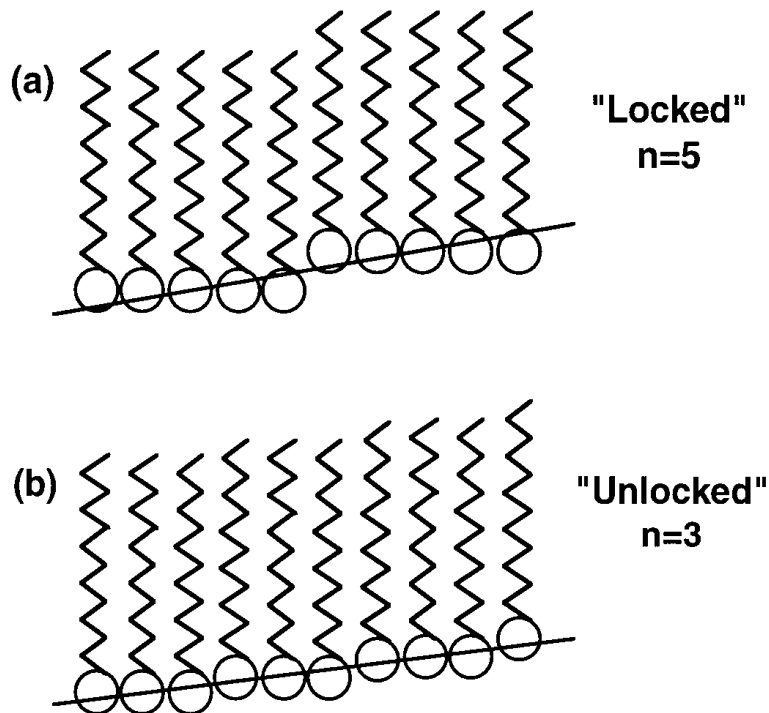


**Figure 8.** Examples of trial solutions for  $\tan\theta = 1/5$  show qualitatively different modulated structures which might occur. (a) The locked structure has four  $0$ -neighbors and one  $+1$ -neighbor. (b) The unlocked modulation has two  $0$ -neighbors and one set of neighbors (per modulation) that doesn't satisfy alkane packing preferences at all.

For simplicity we take special values of  $\theta$  such that  $\tan\theta = 1/D$  for integer values of  $D$ . The energy then becomes:

$$nE = \frac{1}{D^2} \sum_{k=0}^{n-1} \left( k^2 - \frac{n-1}{2} \right)^2 - (n-1)W - \delta_{n,D}W$$

and completing the sum we get

$$E = \frac{n^2 - 1}{12D^2} - \frac{n-1}{n}W - \frac{\delta_{n,D}}{n}W.$$

So, for any given values of  $W$  and  $D$  (which gives  $\theta$ ) we can explicitly minimize this energy over values of  $n$  to determine the lowest energy periodicity. If  $n \neq D$ , then the "jump" in the sawtooth profile (the  $n$ th neighbor) does not match a preferred alkane packing and we will call it an "unlocked" modulation. If  $n = D$ , then all neighboring molecules satisfy alkane packing requirements and we will call it a "locked" modulation. Figure 9 shows the lowest energy solutions as a function of  $W$  and  $\tan\theta = 1/D$ . For a given value of  $\theta$ , the system is flat for small enough  $W$ . As  $W$  increases, it goes through a number of transitions through the "unlocked" modulations. Finally, there is a discontinuous transition to the "locked" modulation at large  $W$ . Note that the unlocked modulations occur at reasonable values of  $W$  even at very small values of  $\tan\theta$ . This is consistent with the unlocked modulations observed where the density was essentially unchanged from that of ideally packed tails.

Note the symmetry of the phase diagram shown in Figure 9 about the line  $\tan\theta = 1/2$ . It turns out that the solution for the system with  $\theta$  such that  $1/2 < \tan\theta \leq 1$  is analogous to the system with  $\theta'$  such that  $\tan\theta' = 1 - \tan\theta$ . The difference is that the two delta functions are interchanged. For example, the locked modulation for  $\tan\theta = 1/6$  has five  $0$ -neighbors and one  $+1$ -neighbor while the locked modulation for  $\tan\theta = 5/6$  has five  $+1$ -neighbors and one  $0$ -neighbor. When  $\tan\theta = 1$ , there is the uniformly tilted phase with no modulation. For values of  $\tan\theta$  greater than 1, the diagram repeats with  $0$ -neighbors mapped onto  $+1$ -neighbors and  $+1$ -neighbors mapped onto  $+2$ -neighbors.

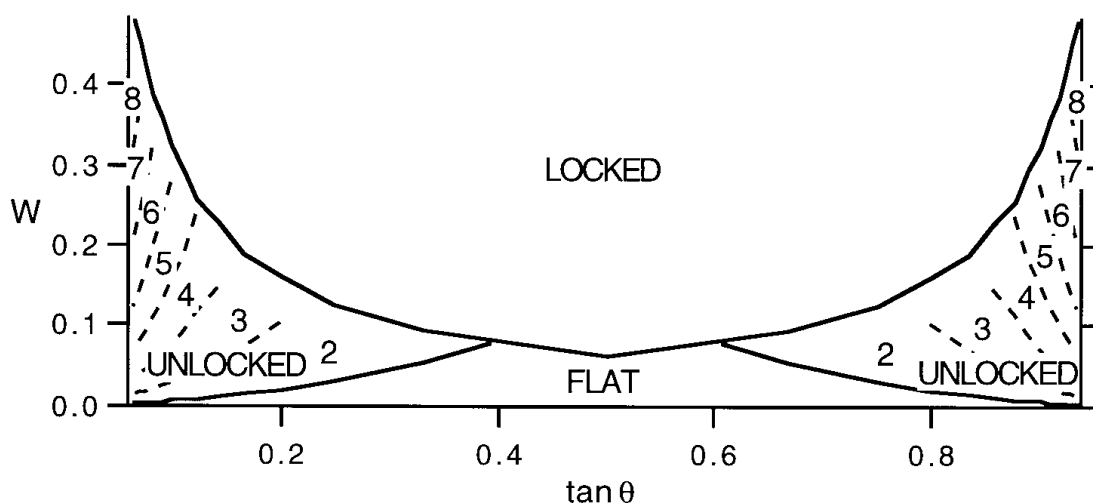


**Figure 9.** The theoretical modulation phase diagram for  $0 \leq \tan\theta \leq 1$ . The model has actually been solved for values of  $\tan\theta$  corresponding to inverse integers. The lines connect the phase boundaries determined at these values.

Monte Carlo simulations were carried out using the full Hamiltonian to test the predictions of the theory. In general, the simulations are consistent with the analytical results. Figure 10 shows the results of simulations carried out for  $D = 10$  at various values of  $W$  (marked as filled circles in Figure 9). As previously mentioned, the simulations justify the sawtooth form of the trial solution. Also, the phase diagram is qualitatively reproduced by the simulations as they demonstrate the progression of structures from flat to  $n = 2$  unlocked to  $n = 3$  unlocked, etc. and eventually to locked ( $n = 10$ ) as  $W$  is increased. However, the simulations suggest several points that were glossed over in the analytical solution because of the simplicity of the assumed trial solution. Firstly, the simulated solutions show substantial disorder in the unlocked phases, especially for higher  $n$ . This is consistent with the disorder observed experimentally. Furthermore, the unlocked structures are locally sawtooth, however, the

periodicity is not always constant. This suggests that the preferred period may not be an integral multiple of the molecular spacing, i.e., it may be incommensurate. The complexity was ignored in the trial solution as only integral wavelengths were considered. Although locked structures only make sense in the context of a commensurate structure, in principle, the unlocked structures could be incommensurate and perhaps the simulations suggest that. A further weakness of the trial solutions used is that no disordered structure is considered.

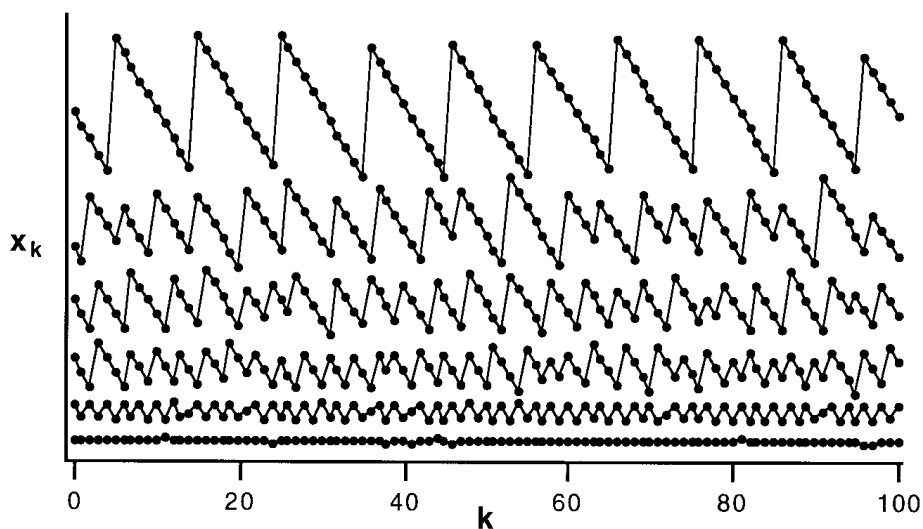


**Figure 10.** Results of Monte Carlo simulations with  $\tan\theta = 1/10$  and  $W = 0.0038, 0.0092, 0.054, 0.13, 0.32,$  and  $1.5$  going bottom to top. The structures are qualitatively consistent with those predicted in figure 9. However, the unlocked structures show significant disorder, increasing with  $W$ .

## 5. Conclusion

In conclusion, atomic force microscopy has allowed quantitative crystallography of the surfaces of LB films. By changing the cation incorporated in the films we were able to change the in-plane density over the range  $18\text{-}20 \text{ \AA}^2/\text{molecule}$ . Except in the extremely close-packed case of  $\text{Pb}^{++}$  the films all contained some type of periodic surface height modulation. Some of the films had "locked" modulations, wherein the defects between uniform regions preserved the close-packing requirements of the alkyl chain tailgroups. These modulations serve to alter the density of the film substantially in order to meet the constraints imposed by the cation/headgroup combination. Other modulations were "unlocked," they were incommensurate with the lattice and had no perceptible effect on the in-plane density.

A model Hamiltonian was constructed that includes the competition between preferred headgroup density and the various discrete tilt angles preferred by crystalline alkane chains. Both Monte Carlo simulations and an analytical solution with a simple sawtooth trial function identify two distinct types of modulations that are consistent with the two types of modulations observed experimentally.

## 6. Acknowledgements

We acknowledge many helpful discussions with C.M. Knobler, R. Granek, W. Gelbart, and Z.-G. Wang. This work was supported by the National Science Foundation and the Office of Naval Research.

## References

1. Israelachvili, J.N., Mitchell, D.J. and Ninham, B.W. (1976) *J. Chem. Soc. Faraday Trans. 2* **72**, 1525.
2. Kitaigorodskii, A.I. (1961) *Organic Chemical Crystallography*, Consultants Bureau, New York.
3. Schwartz, D.K., Viswanathan, R., Garnaes, J. and Zasadzinski, J.A.N. (1993) *J. Am. Chem. Soc.* **115**, 7374.
4. Schwartz, D.K., *et al.* (1993) *Phys. Rev. E* **47**, 452.
5. Zasadzinski, J.A., *et al.* (1994) *Science* **263**, 1726.
6. Schwartz, D.K., Viswanathan, R. and Zasadzinski, J.A.N. (1993) *Phys. Rev. Lett.* **70**, 1267.
7. Schwartz, D.K., Viswanathan, R. and Zasadzinski, J.A.N. (1993) *Langmuir* **9**, 1384.
8. Bourdieu, L., Ronsin, O. and Chatenay, D. (1993) *Science* **259**, 798.
9. Viswanathan, R., Zasadzinski, J.A.N. and Schwartz, D.K. (1994) *Nature* **368**, 440.
10. Schwartz, D.K., Viswanathan, R. and Zasadzinski, J.A. (1994) *J. Chem. Phys.* **101**, 7161.
11. Garnaes, J., Schwartz, D.K., Viswanathan, R. and Zasadzinski, J.A.N. (1992) *Nature* **357**, 54.
12. Schwartz, D.K., Garnaes, J., Viswanathan, R. and Zasadzinski, J.A.N. (1992) *Science* **257**, 508.
13. Scott, H.L. and McCullough, W.S. (1991) *Int. J. Mod. Phys. B* **5**, 2479.
14. Larsson, K. (1977) *Lipids* **20**, 225.
15. Doniach, S. (1979) *J. Chem. Phys.* **70**, 4587.
16. Carlson, J.M. and Sethna, J.P. (1987) *Phys. Rev. A* **36**, 3359.